

# Microstructural characterization of SiC added structural steel

S. Talas\*

*Afyon Kocatepe University, Technical Education Faculty, Afyon 03100, Turkey*

Received 13 December 2005, received in revised form 3 April 2006, accepted 4 April 2006

## Abstract

In this study, the addition of SiC powder to structural steel of SAE 1018 type has been investigated using alloys, which were re-melted in an arc furnace. A systematic addition of SiC resulted in an increase in matrix hardness of the alloys, causing the microstructural constituents being affected by the second phase particles formed as a result of various chemical reactions during re-melting. It is believed that the dissociation of SiC modified the second phase particles in alloys and size distribution profile has been shown to influence the final microstructure of the alloys in favor of high matrix hardness and finer microstructure. These effects were characterized by using standard metallographic techniques.

**Key words:** ferritic steels, microstructure, metal matrix composites (MMC), precipitation

## 1. Introduction

SiC particles, owing to their high hardness and wear resistance property, are widely used to produce high strength-to-weight ratio metal matrix composites [1] and to increase surface hardness and therefore improve wear resistance of steel plates [2]. The use of such particles in steel is commonly utilized since the high solubility of high temperature products of these compounds may substantially change the composition, leading to superior properties of the final product [3]. The surface modification on stainless steel with SiC by laser [2, 4] and powder metallurgy with SiC and various intermetallics [5] and Tungsten Inert Gas melting techniques on low alloy steels modified with Cr and graphite powders [6] have been used for chemical surface modification to expand the use of such commercial alloys. Carbide types of  $M_7C_3$  [6],  $M_{23}C_6$  and  $M_6C$  [2] have been reported on account of increasing hardness in chemically modified layers obtained on stainless and low alloy steels.

In this study SiC, in the form of powder, was added into structural steel and re-melted by arc melting method. The effect of SiC is investigated on plain carbon steels in order to seek possibility to produce steel + SiC composite.

## 2. Experimental procedure

Commercially available SiC powders with an average size of 10  $\mu\text{m}$  were mixed with industrial quality structural steel (SAE 1018) and re-melted in an arc furnace on a water-cooled copper substrate. Spectroscopy results of the structural steel used in this experiment are given in Table 1; steel contained less than 0.704 wt.% impurities of which  $< 0.02\%$  is S. Average cooling rate was timed at 4°C/s. A steel bar of 1 cm diameter and 1.6 cm length was blind-drilled for SiC filling and tapped with the same quality of structural steel. Arc melting was carried out using tungsten electrode of 6 mm diameter under conditions of 65 A and 35 V arc current and voltage, respectively. The total melting time for a complete melting was 45 s for all specimens. The specimens were then sliced and subjected to metallographic examination; 3 vol.% nital was used to reveal the microstructures. The second phase particles were examined using LEO Scanning Electron Microscope (SEM) attached with windowless Quantax EDS (Electron Dispersive X-ray Spectrometer) analyzer. The size distribution of the second phase particles was determined from SEM images obtained from polished and etched specimens using ImageJ software. For hardness tests, 1 kg load and 15 s dwelling time with Vickers tip were employed us-

\* Tel.: +90 272 2281312; fax: +90 272 2281319; e-mail address: stalas@aku.edu.tr

ing Shimadzu HMV microhardness tester. Specimen codes and corresponding SiC additions with final nominal alloy compositions are given in Table 1. Nominal compositions of alloys studied were determined using windowless Quantax EDS attachment due to specimen size limitation. The areas selected for the determination of alloy composition were accounted for approximately 2 % of total surface area for each specimen. The measurements were taken from at least 5 different locations using field scanning method.

### 3. Results and discussion

Metallographic analysis produced no visible macrosegregation effect within the solidified melts. In Fig. 1, the second phase particles in all specimens appear to be well distributed within the melt due to Marangoni and arc forces acting during the re-

Table 1. Specimen codes and final compositions of the alloys and structural steel in wt.%. (Steel contains 98.24 % Fe and < 0.70 % impurities, of which < 0.02 % is S)

Codes	SiC (%)	C	Mn	Si	Bal.
FeSiC1	0.01	4.12	1.46	0.34	NA*
FeSiC10	0.1	6.79	1.16	0.19	NA*
FeSiC20	0.2	7.11	1.45	0.16	NA*
Steel	–	0.19	0.86	0.23	98.94 (Fe+impurities)

\* Not Applicable

melting process. As seen in Table 1, the amount of C is markedly high; this is probably because of the presence of carbides and/or graphite precipitated in large numbers within the matrix. Figures 1a, b and Table 2 show that the addition of SiC caused a significant change in size distribution and also resulted in

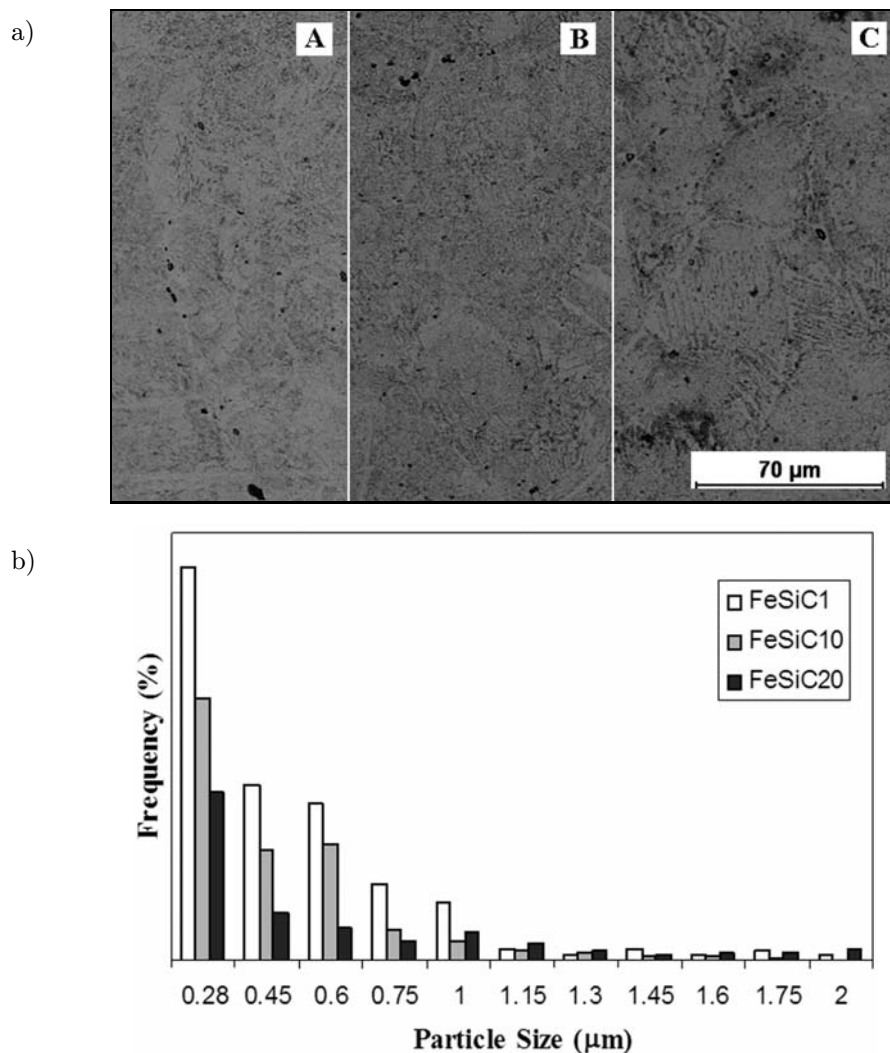


Fig. 1. a) SEM images of SiC containing structural steel specimens A – FeSiC1, B – FeSiC10, C – FeSiC20, b) the frequency (%) of second phase particles vs. particle size (μm) in all series.

a high area fraction ( $a$  (%)) of second phase particles. The drop in frequency of finer second phase particles is the most prominent in FeSiC20 compared to other series, that is, the coarsening of particles seems to be an active process. However, the formation of small particles is probably responsible for increasing the microhardness of matrix at lower SiC additions while the mechanism for a high microhardness at higher additions of SiC can be attributed to an increased number of large particles, which have a high hardness.

The presence of smaller particles (Fig. 1b) indicates that SiC dissolved in the matrix but the precipitation and/or the retention of original carbide of Si was not favored. The precipitation of carbides of Fe is likely since EDS results indicated large amounts C, but very low Si, which is the likely result of a deoxidation process during which Si forms a compound with free O available in the melt, possibly  $\text{SiO}_2$ . Various chemical reactions can take place during re-melting process; the dissociation products of SiC, Si and C may interact with Fe, Mn and S present in the steel to form complex compounds containing C, which is possibly in the form of graphite. It is suggested by some authors [2, 7] that the formation of complex carbides of Fe and Si is likely, such as  $\text{M}_6\text{C}$ ,  $\text{M}_7\text{C}_3$  and  $\text{M}_{23}\text{C}_6$  in the presence of carbide formers. For reactions other than carbides Tahawari et al. [2] suggested the formation of silicides of Fe such as FeSi,  $\text{Fe}_2\text{Si}$  and  $\text{Fe}_3\text{Si}$  from  $\text{SiC}_p + \text{Fe} \rightarrow \text{Fe}_x\text{Si}_y + \text{C}$  reaction. EDS analysis from a second phase particle in FeSiC1 (Fig. 2) suggests that the composition of these particles is rather complex and contains large amount of C and Si. A likely combination of complex compounds could be (Fe, Si)C.MnS or  $\text{SiC.MnS} + \text{C}$ .

Table 2. Specimen codes and corresponding hardness (HV 1 – Vickers scale with 1 kg) (The average hardness and average particle size in as sold condition are 278 HV 1 and  $0.64 \mu\text{m}$ , respectively), average particle size values,  $d$ , and the area fraction of particles  $a$  (%)

Code	Hardness	$d$ ( $\mu\text{m}$ )	$a$ (%)
FeSiC1	572 (HV 1)	0.98	0.65
FeSiC10	615 (HV 1)	1.12	1.2
FeSiC20	685 (HV 1)	1.36	1.9

Dark microstructural features in Fig. 1a indicate a localized compositional change, which is likely to be the result of an increase in C. The high solubility of C in austenite may have produced martensite that is etched darker than the remaining ferrite matrix. This compositional change within the matrix also contributes to increased hardness together with a high cooling rate. As seen in Fig. 3, the microstructural development appears to be assisted by the second phase particles acting as nucleation sites for secondary ferrite plates. The compounds, such as oxides and nitrides [8, 9] of Ti, are well known to play a role in the formation of (acicular) ferrite plates in low C low-alloyed steel welds. The effects of such compounds are studied in steel welds with the purpose of relating the potency of nucleation, which is a measure to define the effectiveness of inclusions to nucleate ferrite during solid state transformation [10] and the solidification of Fe [11]. The inert substrate theory proposed by Dowling et al. [7] states that inclusions formed during the

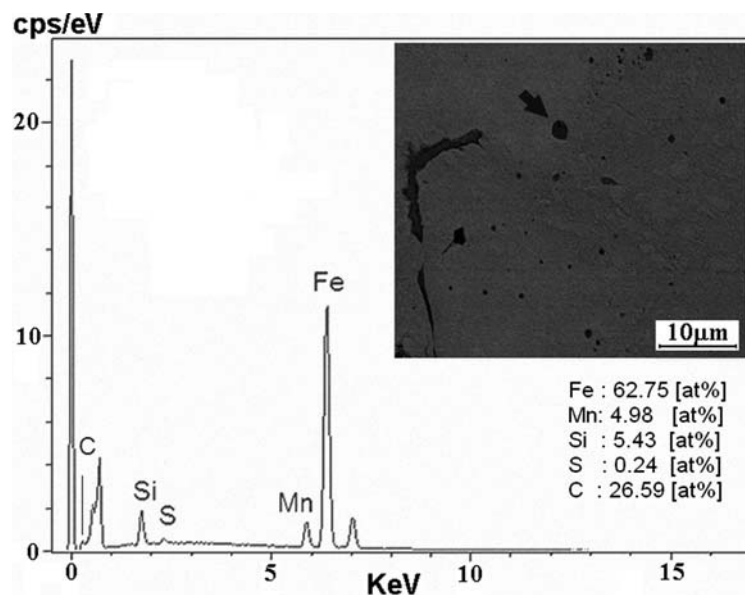


Fig. 2. EDS analysis result from a second phase particle in FeSiC1.

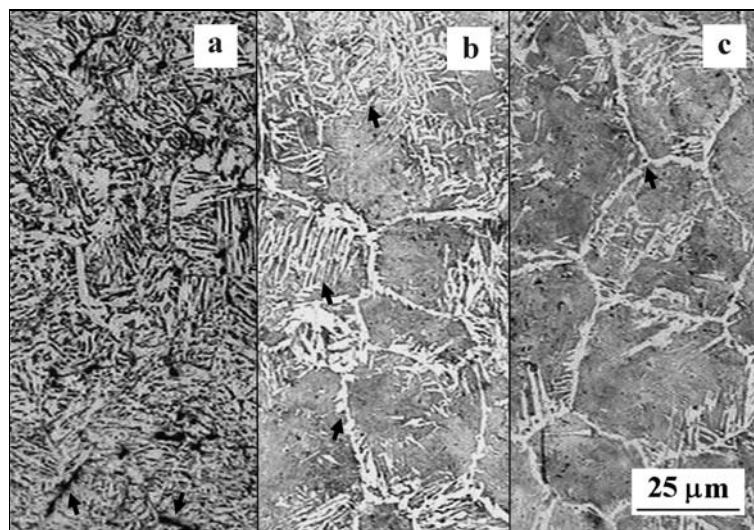


Fig. 3. Optical microscopy images of a) FeSiC1, b) FeSiC10 and c) FeSiC20.

welding process may act as inert substrates to lower the thermal driving force necessary to nucleate ferrite. Such decrease in the free energy of formation results in a high percentage of acicular structure within austenite grain in competition with grain boundary ferrite and ferrite side plates. Regarding the formation of secondary ferrite plates in this study, the complex compound of Fe and C may have acted as heterogeneous nucleation site for ferrite transformation from austenite phase. Figure 3a shows the segregation of carbides located at the boundaries of grains containing ferrite side plates and bainite. The absence of the grain boundary ferrite indicates that the size and number distribution of second phase particles inside the grain is either ineffective as nucleation sites for primary ferrite or a reduced boundary energy due to the presence of a thin layer of carbide (shown by arrows in Fig. 3a) makes it less favorable for ferrite to nucleate at grain boundary. The carbides in the form of layer at grain boundaries are seen when the level of Si is not sufficient to suppress the formation of cementite [12].

As seen in Fig. 3b, the microstructure consists of large grains decorated with grain boundary ferrite. The acicular structure of ferrite, shown by arrow (top), is clearly distinguished and the remaining is martensite supersaturated with C and ferrite side plates (middle arrow) emerging from the grain boundary, assisted by the partitioning of C into austenite at relatively higher temperatures. The presence of second phase particles, carbides, at the grain boundaries (shown by arrow (bottom) in Figs. 3b and 3c) aided the formation of primary ferrite phase during the course of austenite to ferrite transformation. The precipitation of carbide occurs rapidly from austenite which is supersaturated with C and has a maximum solubility of 2.1 wt.% C, reducing C content of austen-

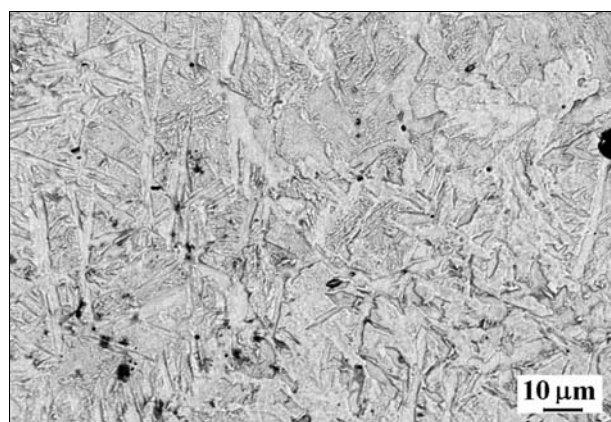


Fig. 4. A SEM image from FeSiC10 showing ferrite plates nucleated on C rich particles with a matrix composed of martensite.

ite phase and increasing the free energy of formation of ferrite as a result of increased diffusivity of C. First, the formation of grain boundary ferrite is eventually favored and secondly, intragranularly formed carbides act as an inert substrate, lowering the driving force for the formation of ferrite plates in some grains (Fig. 4). The mean effective particle diameter is  $0.85 \mu\text{m}$  but a secondary phase particle as large as  $1.3 \mu\text{m}$  in diameter was also seen to nucleate ferrite plate. This is contrary to a previous report [13] where the authors claimed that inclusions smaller than  $0.56 \mu\text{m}$  and larger than  $0.81 \mu\text{m}$  are not classified as efficacious for nucleating ferrite. However, Harrison [14] and Liu and Olson [15] reported results in line with the current work. The appearance of secondary ferrite plates, with sharp tip ends and high aspect ratio, implies that the growth mechanism is non-diffusional; they grow in austenite supersaturated with C until the impingement of ferrite

plates and a cessation in reaction to allow C diffusion to austenite. Grains with relatively low numbers of intragranular inert substrates, i.e. carbides or second phase particles, nucleate little or no ferrite plates and the remaining austenite transforms into martensite. It is also possible to assume that the enrichment of C in the vicinity of ferrite plates is higher relative to austenite which, when supersaturated with C, ceases the advancement of ferrite plates and the reaction ends with the displaceable transformation of martensite.

#### 4. Conclusions

The addition of SiC to structural steel gave rise to unique microstructures, which included retained austenite, martensite and acicular-like ferrite. The amount of second phase particles (carbides of Fe and probably Si in various combinations) increased with increasing SiC addition. The substantial dissociation of the original carbide (SiC) into elemental Si and C resulted in an increase in C in the alloy, which further stabilized the austenite. This led to subsequent formation of martensite that is useful to increase the hardness of steel.

#### Acknowledgements

This work has been supported by the Scientific Research Council of Afyon Kocatepe University, Turkey. The author also thanks Dr. S. Banerjee for critically reading the manuscript.

#### References

- [1] ABBAS, G.—GHAZANFAR, U.: *Wear*, 258, 2005, p. 258.
- [2] THAWARI, G.—SUNDARARAJAN, S. V.—JOSHI, S. V.: *Thin Solid Films*, 423, 2003, p. 41.
- [3] PUTATUNDA, S. K.: *Mat. Sci. Eng.*, A297, 2001, p. 31.
- [4] WOLDAN, A.—KUSINSKI, J.—TASAK, E.: *Mater. Chem. Phys.*, 81, 2003, p. 507.
- [5] ABENOJAR, J.—VELASCO, F.—TORRALBA, J. M.—BAS, J. A.—CALERO, J. A.—MARCE, R.: *Mat. Sci. Eng.*, A335, 2002, p. 1.
- [6] EROGLU, M.—OZDEMIR, N.: *Surf. Coat. Tech.*, 154, 2002, p. 209.
- [7] DOWLING, J. M.—CORBETT, J. M.—KERR, H. W.: *Metall. Mater. Trans.*, A17, 1986, p. 1611.
- [8] TALAS, S.—COCHRANE, R. C.: *Microsc. Microanal.*, 9 (Suppl. 2), 2003, p. 698.
- [9] GREGG, J. M.—BHADESHIA, H. K. D. H.: *Acta Mater.*, 45, 1997, p. 739.
- [10] SHIM, J.-H.—OH, Y.-J.—SUH, Y.-J.—CHO, Y. W.—SHIM, J.-D.—BYUN, J.-S.—LEE, D. N.: *Acta Mater.*, 49, 2001, p. 2115.
- [11] BRAMFITT, B. L.: *Met. Trans.*, 1, 1970, p. 1987.
- [12] PUTATUNDA, S. K.: *Mat. Design*, 24, 2003, p. 435.
- [13] TERASHIMA, A.—HART, P. H. M.: In: *Proceedings The effect of residual, impurity and microalloying elements on weldability and weld properties*. Eds.: Dolby, R. E., Hart, P. H. M. London, The Welding Institute 1983, p. 22.
- [14] HARRISON, P. L.: *Continuous cooling transformation, kinetics and microstructure of mild and low-alloy steel weld metals*. [PhD Thesis]. University of Southampton, 1982.
- [15] LIU, S.—OLSON, D. L.: *Weld J. Res. Suppl.*, 65, 1986, p. 139.